**ATOMIC ENERGY
OF CANADA LIMITED**
Research Company

**ÉNERGIE ATOMIQUE
DU CANADA LIMITÉE**
Société de Recherche

GROUNDWATER CHEMISTRY AND FRACTURE MINERALOGY IN THE WHITESHELL RESEARCH AREA: SUPPORTING DATA FOR THE GEOSPHERE AND BIOSPHERE TRANSPORT MODELS

CHIMIE DES EAUX SOUTERRAINES ET MINÉRALOGIE DES FRACTURES DE L'AIRE DE RECHERCHES DE WHITESHELL: DONNÉES D'APPUI DES MODÈLES DE MIGRATION DANS LA GEOSPHÈRE ET LA BIOSPHÈRE

M. Gascoyne, D. C. Kamineni

DISCLAIMER

Portions of this document may be illegible in electronic image products. Images are produced from the best available original document.

NOTICE

This Technical Record covers ongoing work done as part of the Nuclear Fuel Waste Management Program, and is intended for quick dissemination of the information. The information it contains may not yet have been evaluated rigorously, and any conclusions may be subject to modification in the light of further work.

The report is not to be listed in abstract journals. If it is cited as a reference, the source from which copies may be obtained should be given:

Scientific Document Distribution Office (SDDO),
AECL Research
Chalk River, Ontario KOJ 1J0.

Please refer to the TR-number when requesting additional copies of this document. Single copies of this report are available at no charge from SDDO.

GROUNDWATER CHEMISTRY AND FRACTURE MINERALOGY IN THE
WHITESHELL RESEARCH AREA: SUPPORTING DATA FOR THE GEOSPHERE AND
BIOSPHERE TRANSPORT MODELS

by

M. Gascoyne and D.C. Kamineni

ABSTRACT

For the case study in the Environmental Impact Statement for the Canadian
Nuclear Fuel Waste Management Program, segments of the geosphere transport
model (GEONET) have been assigned groundwater chemical properties and
mineralogical abundances based on data obtained from analysis of ground-
waters and rock types in the Whiteshell Research Area. For the ground-
waters, salinity and redox conditions range from 0.5 g/L and +200 mV for
the shallowest to 25 g/L and -300 mV for the deepest rock layers in the
model. The salinity and redox trends of the segments are consistent with
observations of other Canadian Shield environments and with concentrations
of redox-sensitive species in the groundwater and fracture mineralogy.
Modal volume percent of minerals estimated from thin sections of core
samples have been used as input data for the same segments of GEONET. The
most common minerals include chlorite, muscovite, clays (mainly illite),
calcite and iron oxides. In addition, iodide concentrations for these
segments have also been determined from available data to provide support-
ing data for the biosphere transport model (BIOTRAC). The concentrations
range from 5 μg/L for shallow to 350 μg/L for deep groundwaters. Likely
iodide concentrations for well water or near-surface water discharging into
a lake in BIOTRAC range from 5 to 70 μg/L depending on well depth. A uni-
form probability distribution function is regarded as most appropriate for
the groundwater data inputs and a normal distribution is most suitable for
the mineralogical modal percent composition.

MASTER

CHIMIE DES EAUX SOUTERRAINES ET MINÉRALOGIE DES FRACTURES

DE L'AIRE DE RECHERCHES DE WHITESHELL: DONNÉES D'APPUI

DES MODÈLES DE MIGRATION DANS LA GEOSPHÈRE ET LA BIOSPHÈRE

par

M. Gascoyne et D.C. Kamineni

RÉSUMÉ

Pour l'étude de cas du Dossier d'impact sur l'environnement dans le cadre du Programme canadien de gestion des déchets de combustible nucléaire, on a affecté à des segments du modèle de migration dans la géosphère des propriétés chimiques d'eaux souterraines et une abondance de minéraux basés sur les résultats de l'analyse des eaux souterraines et des types de roches de l'Aire de recherches de Whiteshell. Dans le cas des eaux souterraines, la salinité et les conditions redox s'échelonnent de 0,5 g/L et +200 mV des strates de roche à la profondeur la plus faible à 25 g/L et -300 mV des strates de roche à la profondeur la plus grande représentées par le modèle. La tendance à la salinité et aux conditions redox des segments correspond à celle du bouclier canadien ainsi qu'à la concentration d'espèces sensibles aux conditions des eaux souterraines et minéraux de fractures. On a utilisé la composition modale en pourcentage volumique des minéraux évaluée à partir de lames minces de carrottes comme données d'entrée des mêmes segments de GEONET. Les minéraux les plus communs sont la chlorite, la muscovite, les argiles (surtout l'illite), la calcite et les oxydes de fer. De plus, on a déterminé la concentration d'iodure de ces segments à partir de résultats existants afin de fournir des données d'appui du modèle de migration dans la biosphère (BIOTRAC). La concentration s'échelonne de 5 μg/L dans le cas des eaux souterraines à grande profondeur à 350 μg/L dans le cas des eaux souterraines à faible profondeur. Il est probable que la concentration d'iodure pour les eaux de puits et les eaux proches de la surface se déversant dans un lac de BIOTRAC, s'échelonne de 5 à 70 μg/L selon de la profondeur du puits. On considère qu'une fonction de distribution de probabilité uniforme convient le plus aux données d'entrée sur les eaux souterraines et qu'une distribution normale convient le plus à la composition modale en pourcentage des minéraux.

CONTENTS

1. INTRODUCTION

AECL Research has been assessing the concept of deep geological disposal of nuclear fuel waste in plutonic rock of the Canadian Shield as part of the Canadian Nuclear Fuel Waste Management Program, a research and development program begun in 1978 and jointly funded since 1988 by AECL and Ontario Hydro under the auspices of the CANDU Owners Group.

The results of the assessment will be presented in the form of an Environmental Impact Statement (EIS) submitted to a Federal Environmental and Review Office panel. A major component of the EIS is a case study illustrating the methodology for analyzing the long-term performance of a disposal vault after it is closed (postclosure environmental and safety assessment).

In the postclosure environmental and safety assessment, estimates of risk to people and impacts to the environment from contaminants escaping from a disposal vault are made using a systems assessment computer program (SYVAC, Dormuth and Sherman 1981). SYVAC has separate modules that represent components of the system. For the case study the components are a Vault Model, used to estimate the net transport of contaminants released from the disposal vault into the surrounding rock (the geosphere); a Geosphere Model, used to estimate the net transport of contaminants through the rock surrounding the vault to different discharge points at the surface or near-surface; and a Biosphere Model, used to estimate concentrations of contaminants in the soil, water and biota.

The Geosphere Model used in the case study was developed using data obtained from investigation of AECL's Whiteshell Research Area (WRA) and most of the data was derived from the Underground Research Laboratory (URL) lease area (Figure 1). At the URL, the rock near surface contains moderately spaced, near-vertical fractures that die out with depth. The groundwater flow is controlled primarily by low-dipping intensely fractured zones. The interpretation of the geological conditions and its representation for groundwater flow analysis using a three-dimensional finite element code (MOTIF, Guvanasen 1984) are illustrated in Figure 2. Flow and transport calculations using MOTIF identified pathways for the migration to surface discharge areas of contaminants released from various locations in the hypothetical vault.

The Geosphere Model represents important pathways as a three-dimensional array of one-dimensional segments in a transport code (GEONET, Reid et al. 1989). The array is shown viewed from the side in Figure 3. In order to adequately represent the variation in conditions that are known to occur in the field, each segment is assigned properties that are considered appropriate based on the field and laboratory data for the portion of the rock represented by that segment.

In this report we provide the rationale for the assignment of groundwater chemical properties and mineralogical abundances to the GEONET segments in the WRA Geosphere Model used in the case study.

2. PARAMETERS

The hydrogeochemical and geochemical data required for the performance assessment case study of a used nuclear fuel waste disposal vault based on the data from the WRA include estimates of the salinity (or total dissolved solids content, TDS) and redox potential of groundwaters and relative concentrations of rock-forming minerals along groundwater flow paths represented by segments in the geosphere transport model, GEONET. Rock layer nomenclature shown in Figure 3 is derived from Reid et al. (1989). Hydrogeochemical data are used in adjusting groundwater flow rates for density differences; modifying radionuclide sorption coefficients for variation due to ionic strength; and defining likely redox potentials for areas in the groundwater flow path so that appropriate sorption coefficients can be selected. In addition, to allow calculation of radiation dose from ^{129}I to users of water from critical pathways (principally those drawing water from a shallow well), an estimate of natural iodide (I^-) in the well water is required as an input to the biosphere transport model, BIOTRAC (Zach and Sheppard 1992). These parameters must also be assigned probability distribution functions (PDFs) that best describe the expected variation of their values over a given range.

Fracture-filling minerals represent another important input component to GEONET as they may play a significant role in retarding the migration of radionuclides through sorption (Kamineni et al. 1983, 1986; Ticknor et al. 1989). In addition, some specific minerals, iron oxides for example, are likely to control redox reactions in groundwater for certain radionuclides, such as Tc, Se, Pu and Np. In view of this, it is essential to provide information on the nature, composition and amounts (volume percent) of various minerals present, particularly for those segments of GEONET representing fracture zones.

3. SOURCES OF DATA AND METHODS

The hydrogeochemical data have been obtained by analysis of groundwaters sampled from boreholes drilled in the URL lease area, near Lac du Bonnet, southeastern Manitoba, and selected from borehole zones in permit areas in the surrounding WRA (Figure 1). The groundwaters have been sampled from depths of up to 1 km from 1979 to the present. The basic data are contained in a summary spreadsheet WRACHEMF, described by Gascoyne et al. (1992). Values for TDS (in mg/L or its equivalent kg/m³) were obtained by simple summation of ionic content of each groundwater. Redox conditions were determined from a combination of

1) direct electrochemical measurements as Eh (the techniques are described by Ross and Gascoyne (1992), and Ross et al. (1992)) in either a sealed cell at the surface or a down-borehole, in situ sensor;

2) knowledge of redox-sensitive-species concentrations in the groundwater; and

3) the dominant iron-containing mineral present in the flow pathway.

Iodide concentrations were determined by a wet-chemical analytical technique described in APHA (1985). The detection limit is about 1 μg/L and analytical precision is about +5%.

Study of fracture minerals and the rock matrix in the research area was initiated in 1980, and various aspects of this work have been reported by Kamineni et al. (1984, 1986), Stone et al. (1984) and Brown et al. (1992).

Core samples were collected from a number of boreholes intersecting various fracture zones in the URL lease area to characterize the fracture-filling minerals and unaltered- and altered-rock compositions. Four methods have been used to characterize them:

1) Mesoscopic examination to identify the minerals using conventional diagnostic physical properties, such as form, hardness, colour and reactivity with dilute acid.

2) Identification of clay minerals by X-ray diffraction, especially when they occur as thick (1 to 10 mm) infillings.

3) Petrographic examination of fracture-filling minerals that occur as thick ($\geq$5 cm) horizons in cataclastic zones. Polished sections of selected samples were prepared to determine the composition of various minerals through electron microprobe analysis. This analysis provides support for identifications performed by optical microscope techniques. The analysis was carried out on a MAC electron microprobe equipped with a KEVEX energy dispersive spectrometer. Natural mineral standards were used and the analytical raw data were corrected for background, non-resolution, and matrix effects following the procedure of Colby (1980). The details of the microprobe analytical procedure are given by Plant and Lachance (1973).

4) Scanning electron microscopy using an ETEC model coupled with energy dispersive spectrometer and a QUANTIMET analyzer. This technique gives information on morphology of minerals in natural samples, size of minerals to a submicroscopic level and an estimate of volume percent of various minerals on a polished thin section (QUANTIMET only).

4. RESULTS

The flow segments in GEONET (Figure 3) have been grouped into six chemical property classes: a Lower Rock Layer (unfaulted and generally unfractured rock matrix), an Intermediate Rock Layer (unfaulted but somewhat fractured rock matrix), an Upper Rock Layer (unfaulted but with well-developed intersecting sets of fractures) and the sections of Fracture Zone LD1 (see Figure 3) that lie within each of these rock layers. Flow segments in each class are assumed to have the same groundwater chemistry and mineralogical composition. These assumptions are derived from observed changes in groundwater composition for inclined fracture zones in the WRA and from variation of rock type and mineralogy with depth (Gascoyne et al. 1992).

4.1   HYDROGEOCHEMISTRY

A summary of salinity (as TDS), redox potential and iodide content of WRA
groundwaters is shown in Table 1. Also shown are borehole zones, depths
and dates of sampling.

The necessary range of values for the specific intervals in GEONET are
obtained using data from outside the principal flow segments in GEONET.
This is because some indication of the direction of observed trends seen in
URL lease area groundwaters (the centre of the GEONET simulation) are
needed to supplement the limited data available for depths below 400 m at
the URL. For the most part, however, hydrogeochemical data from Fracture
Zones (FZ) 1 and 2 at the URL are used to describe the compositions of LD1
and LD0 respectively.

The variation of salinity, Eh and iodide content with mean sampling depth
is shown in Figures 4 to 6. Trends of increasing salinity and iodide con-
tent, and decreasing Eh with increase in depth can be seen. A more dis-
tinct relationship between iodide and TDS is shown in Figure 7, indicating
that iodide concentration is controlled mainly by salinity.

Value ranges of salinity, redox (as Eh) and iodide have been selected for
each of the chemical property classes of GEONET (Table 2). For the more
saline waters, the I^-/TDS ratio is remarkably constant, varying between
1.2×10^{-5} and 1.6×10^{-5}. This relationship is used to estimate likely
iodide concentrations in the deeper flow segments of the GEONET model and
derive likely concentrations in well water for the BIOTRAC model.

4.2   MINERALOGY

Modal volume percent of minerals has been estimated in the fracture zone
flow paths using 150 thin sections of fracture zone samples. The mean
compositions and standard deviations are given in Tables 3, 4 and 5. The
mineralogical composition of the rock matrix is determined by the same
method as reported by Stone et al. (1989). Although the volume percent of
minerals was determined by visual estimates in this procedure, the results
compare favourably with other methods such as conventional point counting
and the more recently available technique, QUANTIMET, as shown in Table 6.
In this test, the three methods were applied to a polished section.

The most common minerals encountered in fractures and fracture zones in the
WRA include clays, chlorite, muscovite, calcite and iron oxides (goethite-
hematite). X-ray work confirmed illite to be the predominant clay mineral.
A number of other minerals, including laumontite, prehnite, epidote and
gypsum, were identified in some samples, but they occur in minute quanti-
ties and are thus considered to play an insignificant role in radionuclide
sorption.

Microprobe analyses have concentrated mainly on minerals that show variable
stoichiometry. Their occurrence and compositional characteristics are
described below.

Chlorite is present sporadically in the wall rock adjacent to fracture
zones but becomes abundant within the fracture zone, frequently filling the

anastomosing network of minor fractures. In the wall rock, it generally occurs as an alteration product of biotite. The composition of chlorite shows variation in terms of Si, Al, Fe and Mg (see Table 7). The water content, which can be determined by difference, varies between 13 and 15% and is well within the range of normal chlorites (Deer et al. 1966). In terms of the classification scheme of Hey (1954), the chlorites overlap the ripidolite-pychnochlorite-diabantite fields. The grain size of chlorites measured by optical micrometer ranges from 0.04 to 0.006 mm.

Muscovite and/or sericite are common minerals in fracture zones and wall rock. These are formed by alteration of feldspars and are also found along grain boundaries because of interaction during early stages of faulting. These minerals invariably contain sufficient Fe and Mg (see Table 8) to classify them as phengite (Velde 1965). The grain size of muscovite/ sericite varies from 0.03 to 0.005 mm.

Illite occurs as a fracture filling and also as an alteration product on feldspar surfaces. The latter paragenesis is common in regions of intense fluid activity. Between the two feldspars (plagioclase and microcline), plagioclase is the first to be altered to illite, whereas microcline is affected only during extreme cases of alteration. The grain size of illite, determined by SEM, ranges from 0.0003 to 0.0018 mm, and its compositional characteristics are given in Table 8.

Iron oxide is a predominant mineral throughout the fracture zones. It has at least two modes of occurrence:

1) as a coating on feldspars, and

2) as a residual product in fracture zones through alteration of chlorite.

Production of iron oxides through breakdown of chlorite is the most common mode of formation and can be positively confirmed in domains containing various stages of chlorite alteration and pseudomorphs of hematite replacing chlorite flakes. In fracture zones where there is intense fluid activity, the chlorites are completely altered to iron oxides. Compositionally, the iron oxides are homogeneous with minor amounts of Ti and Mn. The grain size is highly variable, ranging from 0.02 to 0.0008 mm.

Calcite is present in almost all fractures and dominates in high-dip fractures (50 to 75°) prevalent at shallow depths in the URL lease area. The grain size of calcite ranges between 0.50 mm to 0.005 mm. Compositionally, calcites are pure $CaCO_3$ and no other components are identified within the limits of resolution of the microprobe. Other carbonates, e.g., siderite ($FeCO_3$), are identified in a few fractures, but they are extremely rare.

4.3 DETERMINATION OF INPUT DATA FOR GEONET AND BIOTRAC

The rationalization for selection of the hydrogeochemical and mineralogical data for GEONET and BIOTRAC is given below, according to chemical class of the flow segment.

4.3.1   Lower Rock Layer (300-500 m)

The TDS concentration for this layer (Table 2) represents a probable value
for the rock matrix. Few direct data have been obtained on soluble rock
matrix salts or the availability of these salts to penetrating solutions
although some results of crush-leach tests on various altered and unaltered
granitic rock types (Gascoyne et al. 1989) have indicated the presence of
soluble chloride salts in the granite matrix. The higher values in the
concentration range of layer 3 in Figure 4 have been selected as represen-
tative of this layer in view of the qualitative evidence that indicates
that rock-matrix salts may contribute to groundwater salinity in the frac-
ture zones (Gascoyne et al. 1989). An Eh value of -300 mV is chosen for
this layer based on the fact that magnetite is present in the rock matrix
(the magnetite-hematite redox boundary lies between -200 and -250 mV in the
pH range 7-8.5).

Because the flow in this layer (in contrast to fracture zone LD1) is pri-
marily through interconnected pore space, retardation factors would be
controlled by sorption coefficients for radionuclides on the inter-
connected pore surfaces. Actual K_d (sorption coefficient) values of grey
granite from the WRA are used for this layer, we have coded it as grey
granite, rather than coefficients based on the mineral components listed in
Table 9.

4.3.2   Fracture Zone LD1 (300-500 m)

The average TDS of groundwater at a depth of 500 m for the WRA is 11.2 g/L
(Gascoyne 1988). This value clearly falls within the distribution in
Figure 4. The mean composition selected for this segment (10 g/L) more
closely reflects the compositions of groundwaters in FZ1 at the URL (depth
range 300-450 m), which tend to be more saline than indicated by the 300-
500 m envelope in Figure 4. The lower value of the Eh range for this layer
(Figure 5) is selected as the most representative because the groundwater
is likely to have been least affected by atmospheric contamination during
measurement. This result is also more consistent with down-hole sensor
measurements (Ross and Gascoyne 1992).

The average volume percent of minerals present in this segment (Table 3) is
obtained by study of samples collected from cored boreholes (URL1 to 8, 10
and 12). The samples represent material recovered from low-dip (<30°)
faults corresponding to FZ1 and FZ2.

4.3.3   Intermediate Rock Layer (150-300 m)

As in the case of the Lower Rock Layer, the composition of matrix solutions
in this layer is assumed to be more saline than that in the fracture zones
and the mean and distribution are taken from the upper part of the Layer 2
envelope in Figure 4. An Eh value of -300 mV is again chosen for this
layer because magnetite is the stable Fe-bearing phase in the rock matrix.

The predominant rock mass in this segment is grey granite, but it generally
has two orders of magnitude greater permeability than the Lower Rock Layer.
As in the Lower Rock Layer, flow in this zone will be through intercon-
nected pores and, hence, a similar approach is adopted here in assigning
the mineralogy (i.e., coded as grey granite).

4.3.4   Fracture Zone LD1 (150-300 m)

No data exists for this level of FZ1 at the URL because it lies outside the property boundary. The assumption is made, therefore, that similar geo-chemical evolutionary processes take place in groundwaters as they flow towards the surface, irrespective of which fracture zone they follow, and FZ2 and its lower splay (FZ1.5) at the URL may be used to determine the composition in LD1 for this layer. The mean value for Eh is chosen to reflect the trend of lower Eh seen in down-hole sensor measurements. These assumptions are supported by measurements in groundwaters from similar depth intervals for boreholes in permit areas elsewhere in the WRA.

This segment contains the same low-dip faults that are encountered in the deeper regions (i.e., 300 to 500 m). Since no mineralogical variation is noted along the dip, the same mineralogical data as those of Fracture Zone LD1 (300 to 500 m) have been chosen (Table 3).

4.3.5   Upper Rock Layer (0-150 m)

Groundwater flow in this layer is defined as occurring through intercon-nected, subvertical fractures containing calcite as the dominant infilling. Although the GEONET simulation only considers discharge flow paths in this layer (so that migration of the plume from the vault may be followed), considerable dilution of the plume occurs by localized recharge through these fractures. Therefore, an average of the data points in the Upper Rock Layer (Layer 1, Figure 4) is used.

In addition to a calcite infilling, many of these subvertical fractures contain slickenlines that are defined by the development of chlorite, which generally disintegrates forming residual minerals (iron oxides). The volume percents of major minerals for this flow segment are given in Table 4.

4.3.6   Fracture Zone LD1 (0-150 m)

Because this part of LD1 is not within the URL property, compositions of FZ3 and near-surface FZ2 groundwaters at the URL are used in the assess-ment. A slightly more saline composition than that of the Upper Rock Layer is chosen for this segment to reflect the fact that LD1 represents the main conduit for groundwater from lower layers with dilution by local recharge in the upper layer. Because of the short travel length and generally more rapid pumping rate, down-hole sensor measurements of Eh suggest that Eh values determined in a surface flowcell are fairly representative and suf-fer little atmospheric contamination. Therefore, no weighting towards lower Eh is given to the mean for this part of LD1.

Iodide concentrations in these dilute groundwaters (TDS < 1 g/L) are vari-able (from ~0 to 17 μg/L) and show no systematic trend with depth, salinity, etc. The lack of trend is probably due to the existence of several sources of iodide (e.g., overburden, vegetation, and rock) that can contribute to the groundwater composition. However, if the GEONET well draws water principally from a bedrock source, iodide concentrations in the water are likely to follow those predicted by the I$^-$/TDS relationship (Figure 7). Iodide concentrations may range, therefore, from 5 to 20 μg/L for a well depth of 100 m and 15-70 μg/L for a depth of 200 m.

Core samples from boreholes (URL1 to 10) intersecting FZ2 and FZ3 at shal-
low depths (0 to 150 m) were used to characterize the mineralogy of this
segment. Again, calcite and iron oxides are the dominant infilling. The
modal volume percent of these minerals is listed in Table 5.

4.4   PROBABILITY DISTRIBUTION FUNCTIONS FOR GEONET AND BIOTRAC

INPUT DATA

A uniform probability distribution function (PDF) is chosen as the most
representative descriptor of variation of salinity, redox and iodide con-
centrations for the six chemical classes in Table 2. This type of PDF
requires that all values within a range be equally probable and all values
outside the range be impossible. The variation of these parameters in
Figures 4 to 6 appears to best follow a uniform distribution and is clearly
not described by constant, normal, piecewise uniform or logarithmic distri-
bution functions (as described, for instance, by Stephens et al. (1989).
Although values outside the given ranges are possible, the ranges have been
chosen to be sufficiently large to encompass all the available data and the
bounds of each range are generally the divisions between the chemical
classes.

The modal volume percent values of mineral abundances best represents a
normal distribution without truncation, except for the physical lower and
upper limits, 0 and 1. The total mineral fraction is considered as an
independent variable within its fractional abundance distribution. After
sampling is done, the values are renormalized to bring the total fractional
abundance to unity.

5. DISCUSSION

The variation of salinities of WRA groundwaters with respect to depth is
similar to that seen in the East Bull Lake and Eye-Dashwa Lakes Research
Areas, and in mine groundwaters from the Canadian Shield (Bottomley et al.
1986, Gascoyne et al. 1987). Possible exceptions to the classifications
shown in Table 2 may arise if saline groundwaters are encountered near the
surface in a fracture zone that carries groundwater from depth, discharging
to the surface with negligible dilution. Such a possibility is one expla-
nation for the "moose lick" springs observed in the Nipigon area of north-
western Ontario (Frape et al. 1984). Alternatively, a steep, deeply pene-
trating fracture may cause recharge of dilute groundwater to considerable
depth. This has been observed in one instance in the Eye-Dashwa Lakes
Pluton (Gascoyne et al., unpublished data). In the region of the WRA, the
only significant anomaly in the salinity-depth relationship is seen in
overburden groundwaters, which may have TDS concentrations as high as 5 g/L
because of the presence of $Na-Ca-Mg-HCO_3-SO_4$ ions, derived from readily
soluble salts and minerals in the clay fraction of the overburden. These
salinities are shown in Figure 4.

Similar trends of decreasing redox potential with depth have also been seen
in other research areas (Gascoyne et al. 1987), but there are few data
available for mine groundwaters. Although the redox values determined for

WRA groundwaters are only derived as Pt electrode potentials, their general range and distribution within the mildly oxidizing to mildly reducing fields is supported by several hydrogeochemical observations:

1) Fe^{3+} is absent and Fe^{2+} is only present in minor amounts (generally <1 mg/L), even in the deepest, most saline groundwaters;

2) Fe-bearing alteration products in permeable fractures are generally in the Fe^{3+} form (i.e., hematite, goethite and amorphous oxyhydroxides);

3) H_2S is absent in all groundwaters except, occasionally, in shallow bedrock or overburden waters, where biological activity may be causing reduction of dissolved SO_4;

4) SO_4 concentrations increase with depth and remain high (~1 g/L) as groundwater salinity increases, indicating no reduction to H_2S or metal sulphides;

5) U contents of WRA groundwaters are high and are seldom lower than 1 μg/L, even in the deepest, most saline groundwaters (Gascoyne 1989), indicating that U solubility is not controlled by the reduced U(IV) species but by the more soluble U(VI) form; and

6) H_2 and CH_4 are generally absent in all WRA groundwaters.

Data on iodide concentrations in WRA groundwaters have only recently become available, and so far only about 40 analyses have been made of all water types (Figures 6, 7). Variations outside the limits described in Table 3, therefore, are quite possible, especially for shallow, low-salinity groundwaters.

The ranges given here for salinity, redox and iodide apply to current conditions and are likely to be applicable as long as there are no major perturbations of the groundwater flow regime (as may occur because of climate changes, glaciation, etc.). Glaciation, for instance, may lead to increased groundwater salinities due to the displacement of dissolved salts as water freezes close to the surface. Redox conditions may also shift between oxidizing and reducing because of variations in the supply of oxygenated surface water. It is impossible, however, to estimate the extent of such changes for the purposes of defining ranges of values for the parameters used in GEONET and BIOTRAC.

The volume percent values for minerals used in the GEONET input code represent data generated from the study of samples collected exclusively from the URL lease area. Subsequent work in other permit areas (A, B, C, D, G and at the WL site, Figure 1) shows that the results listed in Tables 3, 4 and 5 are applicable to the entire WRA. However, certain fracture zones encountered in these permit areas contain epidote as the main fracture-filling mineral, with minor amounts of chlorite and hematite. As this variety of fracture zone is not abundant and, more particularly, is far removed from the block designated for the GEONET analysis, it is not included in the GEONET input data.

6. SUMMARY AND CONCLUSIONS

Salinity and iodide content of WRA groundwaters have been found to increase progressively with depth in the Lac du Bonnet granite batholith. In particular, the increase in iodide is closely related to increasing TDS. Redox potential of the groundwaters, measured as an electrode potential, shows a general decrease with increase in depth. Strongly reducing conditions are not encountered at great depth (~1 km), however, and this is supported by the low Fe^{2+}, H_2S, H_2, CH_4 concentrations and high U, SO_4 concentrations in deep, saline groundwaters. Calcite, chlorite, muscovite, iron oxide and illite are the dominant fracture-filling minerals in the granite of the WRA. The detailed mineralogical composition of the rock matrix and major fracture zones has been determined in terms of modal volume percent abundances. Using the above results, the GEONET flow network has been divided into six segments, each with specified chemical and mineralogical properties, for use in the geosphere and the biosphere transport models illustrating the methodology for assessing the performance of a used nuclear fuel waste vault.

REFERENCES

APHA, AWWA, WPCF. 1985. Iodide: 414B. Catalytic reduction method. Standard Methods for the Examination of Water and Wastewater, 16th Edition, 367-368.

Bottomley, D.J., M. Gascoyne, J.D. Ross and J.J. Ruttan. 1986. Hydrogeochemistry of the East Bull Lake pluton, Massey, Ontario. Atomic Energy of Canada Limited Technical Record, TR-382.

Brown, A., J.J.B. Dugal, R.A. Everitt, D.C. Kamineni, J.S.O. Lau, G.F. McCrank and N. Roy. 1992. Geology of the Lac du Bonnet Batholith, Manitoba. Summary of AECL geological research at RA3. Atomic Energy of Canada Limited Report (in preparation).

Colby, J.W. 1980. MAGIV V - A computer program for quantitative electron excited energy dispersive analysis. Instruction manual QUANTEX RAY. Appendix E, ED-1: 1/8/80. Kevex Corporation, Foster City, CA.

Deer, W.A., R.A. Howie and J. Zussman. 1966. An Introduction to the Rock-Forming Minerals. Part 3: Sheet Silicates. Longman, London, 348 p.

Dormuth, K.W. and G.R. Sherman. 1981. SYVAC - A computer program for assessment of nuclear fuel waste management systems incorporating parameter variability. Atomic Energy of Canada Limited Report, AECL-6814.

Frape, S.K., P. Fritz and A.J. Blackmer. 1984. Saline groundwater discharges from crystalline rocks near Thunder Bay, Ontario, Canada. In Hydrochemical Balances of Freshwater Systems (Eriksson, E., editor), International Association of Hydrological Sciences Publication No. 150, 369-379.

Gascoyne, M. 1988. Reference groundwater composition for a depth of 500 m in the Whiteshell Research Area - Comparison with synthetic groundwater WN-1. Atomic Energy of Canada Limited Technical Record, TR-463.

Gascoyne, M. 1989. High levels of uranium and radium in groundwaters at Canada's Underground Research Laboratory, Lac du Bonnet, Manitoba. Applied Geochemistry 4, 577-592.

Gascoyne, M., C.C. Davison, J.D. Ross and R. Pearson. 1987. Saline groundwaters and brines in plutons in the Canadian Shield. In "Saline Waters and Gases in Crystalline Rocks (Fritz, P. and Frape, S.K., editors), 53-68, Geological Association of Canada Special Paper, No. 33, 53-68.

Gascoyne, M., J.D. Ross, R.L. Watson and D.C. Kamineni. 1989. Soluble salts in a Canadian Shield granite as contributors to groundwater salinity. In Proceedings of the 6th International Symposium on Water Rock Interaction, Malvern, U.K., 1989, 247-249.

Gascoyne, M., J.D. Ross, R.L. Watson and J.P.A. Larocque. 1992. Hydrogeochemistry of the Lac du Bonnet granite batholith, southeastern Manitoba. Atomic Energy of Canada Limited Technical Record (in preparation).

Guvanasen, V. 1985. Development of a finite-element hydrogeological code and its application to geoscience research. Atomic Energy of Canada Limited Technical Record, TR-299, 554-566.

Hey, M.H. 1954. A new review of the chlorites. Mineralogical Magazine 30, 277-292.

Kamineni, D.C., T.T. Vandergraaf and K.V. Ticknor. 1983. Characteristics of radionuclide sorptions on fracture-filling minerals in the Eye-Dashwa Lakes pluton, Atikokan, Ontario. Canadian Mineralogist 21, 625-636.

Kamineni, D.C., J.J.B. Dugal and R.B. Ejeckam. 1984. Geochemical investigations of granitic core samples from boreholes at the Underground Research Laboratory site near Lac du Bonnet, Manitoba. Atomic Energy of Canada Limited Technical Record, TR-221.

Kamineni, D.C., K.V. Ticknor and T.T. Vandergraaf. 1986. Occurrence, composition and radionuclide sorption characteristics of illite from a fractured granite pluton, southeastern Manitoba, Canada. Clay Minerals 21, 909-924.

Plant, A.G. and G.R. Lachance. 1973. Quantitative electron microprobe analysis using an energy dispersive spectrometer. In Proceedings of the Eighth National Conference on Electron Microprobe Analysis, Paper 13, 21-38.

Reid, J.A.K., T.W. Melnyk and T. Chan. 1989. Effects of a domestic well on assessed performance of a nuclear fuel waste disposal system. In Proceedings of NEA/OECD Workshop on Assessment of the Risks Associated with Human Intrusion at Radioactive Waste Disposal Sites, 1989 June 5-7, Paris, France.

Ross, J.D., M. Gascoyne, R.L. Watson and J.P.A. Larocque. 1992. Procedures for the collection, measurement and analysis of groundwaters for the CNFWMP. Atomic Energy of Canada Limited Technical Record (in preparation).

Ross, J.D. and M. Gascoyne. 1992. Comparison of surface and downhole electrochemical measurements in Canadian Shield groundwaters. Atomic Energy of Canada Limited Technical Record, TR-478 (in preparation).

Stephens, M.E., B.W. Goodwin and T.H. Andres. 1989. Guidelines for defining probability density functions for SYVAC3-CC3 parameters. Atomic Energy of Canada Limited Technical Record, TR-479.

Stone, D., D.C. Kamineni and A. Brown. 1984. Geology and fracture characteristics of the Underground Research Laboratory lease near Lac du Bonnet, Manitoba. Atomic Energy of Canada Limited Technical Record, TR-243.

Stone, D., D.C. Kamineni, A. Brown and R. Everitt. 1989. A comparison of fracture styles in two granitic bodies of the Superior Province. Canadian Journal of Earth Sciences 26, 387-403.

Ticknor, K.V., T.T. Vandergraaf and D.C. Kamineni. 1989. Radionuclide sorption on primary and fracture-filling minerals from the East Bull Lake pluton, Massey, Ontario, Canada. Applied Geochemistry 4, 163-176.

Velde, B. 1965. Phengite micas: synthesis, stability and natural occurrence. American Journal of Science 263, 886-913.

Zach, R. and S.C. Sheppard. 1992. The food-chain and dose submodel, CALDOS, for the assessment of Canada's nuclear fuel waste management concept. Atomic Energy of Canada Limited Report AECL-10165, COG-91-195.

TABLE 1

GROUNDWATER CHEMISTRY DATA FOR THE WHITESHELL RESEARCH AREA GEOSPHERE MODEL

(Parentheses indicate analyses for samples taken on different dates to those shown and zone depth refers to the depth below collar of the permeable horizon.)

Sample Name	Approx. Zone Depth (m)	Date	TDS (mg/L)	Eh (mV)	I (μg/L)
C68	2	12-Aug-86	1 501		
102-1	2	06-Aug-87	2 354		
102-2	5	06-Aug-87	1 374		7
103-1	4	24-Jul-87	2 916		28
103-2	6	24-Jul-87	5 266		54
103-3	8	24-Jul-87	4 513		103
112-1	2	06-Aug-87	1 313		16
112-3	5	06-Aug-87	1 193		45
B26-2-3	38	18-Nov-82	272		
B27-2-1	36	19-Aug-82	376		
B34-2-4	40	28-Jul-88	1 493	10	16
B37-1-10	22	16-Sep-83	1 002	131	
B37-2-3	45	31-Jul-87	1 214	52	
B38-1-5	12	21-Jun-83	374		
B38-2-4	35	14-Jun-83	402		
B40-2-1	52	25-Aug-83	517		
B41-1-2	23	12-Aug-83	395		
B41-2-1	48	11-Aug-83	509		
B43-2-3	123	21-Apr-83	334		
M1A-3-1	265	21-Apr-86	722		
M1B-2-3	75	14-Aug-87	341	51	
M2A-3-4	310	29-May-86	354	46	(1.5)
M2B-2-5	150	09-Aug-87	397	37	
M3A-3-4	375	07-Jul-88	5 997		
M3B-2-1	120	29-Jul-87	194	248	17
M4A-1-15	180	02-Dec-83	388		(1.4)
M4A-2-2	215	06-Dec-83	288		
M4A-3-7	260	07-Dec-83	385		
M4A-4-6	310	21-Jul-86	1 616	-26	(23)

TABLE 1 (continued)

Sample Name	Approx. Zone Depth (m)	Date	TDS (mg/L)	Eh (mV)	I (μg/L)
M5A-3	165	12-May-83	867		
M5A-IN8	340	16-Sep-83	7 586	55	
M5B-IN9	120	18-Sep-83	393	19	
M6-2-5	110	07-Aug-86	321	68	4
M7-72-DH	72	31-Oct-83	648	224	
M7-4-11	390	05-Sep-86	14 896	36	470
M8-3-7	360	06-Jun-86	326	40	2
M8-10	140	24-Jun-83	242		
M9-3-3	230	18-Jul-88	287		
M10-1-7	50	11-Nov-88	348		
M10-3-2	410	15-Apr-86	6 017	-4	83
M11-2-12	140	30-Nov-83	337		
M11-3-4	290	21-Jul-88	1 844		
M12-93-DH	93	06-Sep-83	360	-38	
M12-159-18DH	159	26-Aug-83	375	-185	
M12-171-15DH	171	28-Jul-83	377		
M13-2-5	250	17-Jun-86	2 954	-50	36
M14-13	105	27-Jan-84	499		
M14-1-4	50	10-Aug-88	373		
M14-4-4	370	03-Jun-86	11 120	-15	(53)
URL1-24	110	09-Sep-83	219		
URL1-20	320	05-Apr-83	452		
URL2-10	120	13-Jul-82	260		
URL2-11-2	780	15-Aug-89	21 701		423
URL3-5-1	120	02-Dec-83	508	120	
URL3-6-9	140	20-Aug-88	340		
URL4-5-10	65	23-Jul-86	292	160	(3.5)
URL5-43	100	11-May-82	495		
URL6-25	270	12-Jul-83	868		
URL7-24	60	22-Aug-82	280		
URL8-5	70	30-May-84	320		
URL8-6	230	14-Aug-84	377		
URL9-22	110	05-Jul-85	303		
URL10-3-2	80	09-May-86	272	143	
URL10-6-7	250	24-Jun-86	649	66	(5.5)
URL11-1	45	20-Jul-84	279		
URL11-7-7	135	29-Nov-88	370		
URL12-11-13	430	11-Sep-86	413	95	(6.1)

TABLE 1 (concluded)

Sample Name	Approx. Zone Depth (m)	Date	TDS (mg/L)	Eh (mV)	I (μg/L)
URL12-13-21	605	22-Jul-86	4 897	113	55
URL14-8	280	23-Jul-87	6 658	11	(90)
URL15-1-4	125	26-May-88	745	-53	(12.5)
URL16-4-1	85	24-Aug-88	338		
WA1-1-3	150	10-Jul-87	188		
WA1-2-8	240	29-Jun-87	344	-75	
WA1-3-8	320	08-Nov-87	470	-126	
WA1-5-7	630	18-Mar-88	8 028	-124	
WB1-1-5	130	05-Jun-87	465		
WB1-2-6	230	05-Jun-87	1 074	-90	15
WB1-4-SW10	540	05-Aug-87	17 085		
WB1-5-21	630	06-Oct-87	18 528	-290	
WB1-7-7	1000	30-May-88	50 735	-197	
WD1-110-2	100	03-Sep-88	353	-56	
WD2-72-5	65	01-Sep-88	363	96	
WD3-895-10	810	14-Sep-88	18 156	-85	
WG2-2-8	130	15-May-87	319		2
WNP1	19	25-Jul-80	496	85	
WN1-8-17	380	24-May-87	6 935	41	123
WN3-37	37	25-Jul-79	1 014	140	
WN3-90	90	20-Aug-79	729	110	
WN4-6-8	370	08-May-87	7 671	109	142
WN8-T4	315	26-Aug-88	5 142	107	
WN10-3-4	245	09-Dec-88	3 213		
WN10-4-3	320	26-Mar-87	6 655	-126	102
WN11-17-15	1000	09-Dec-86	31 845	45	463
HC9-14	250	22-Nov-88	558		(3)
HC15-Z3-14	310	22-Nov-88	5 622		(58)
HC16-Z3-14	310	22-Nov-88	2 201		
HC21-14	250	22-Nov-88	633		(11)
HC26-Z4-14	310	22-Nov-88	7 315		(132)
HC27-14	250	22-Nov-88	586		(13)
VR-14	200	22-Nov-88	509		
RM.209 DRIP-14	240	22-Nov-88	1 144		(41)

TABLE 2

SELECTED RANGES OF VALUES OF SALINITY (AS TDS), I⁻ AND REDOX POTENTIAL (AS Eh) FOR THE GEONET MODEL

GEONET Segment	Depth (m)	TDS (g/L)		Eh (mV)		I⁻ (μg/L)
		Range	Mean	Range	Most Representative	Likely Range
Lower Rock Layer	300-500	15-25	20	<-300 to -200	-300	210-350
LD1	300-500	5-20	10	<-200 to +100	-200	70-280
Intermediate Rock Layer	150-300	3-13	10	<-300 to -200	-300	40-180
LD1	150-300	1-5	2	-200 to +100	-100	15-70
Upper Rock Layer	0-150	0.3-0.8	0.4	-100 to >+150	+50	5-10
LD1	0-150	0.5-1.5	1	-50 to +200	+50	5-20

TABLE 3

MODAL VOLUME PERCENT OF FRACTURE FILLING MINERALS IN LOW-DIP FRACTURE ZONES (150- TO 500-m DEPTH)

Mineral	vol.%
Chlorite	14 ± 5
Muscovite	3 ± 3
Illite	19 ± 15
Iron oxides	15 ± 9
Calcite	3 + 2
Biotite	5 ± 4
Plagioclase	11 ± 8
Microcline	15 ± 6
Quartz	15 ± 5

TABLE 4

MODAL VOLUME PERCENT OF FRACTURE FILLINGS MINERALS
IN SUBVERTICAL FRACTURES (0- TO 150-m DEPTH)

Mineral	vol.%
Chlorite	25 ± 10
Illite	2 ± 1
Iron oxides	30 ± 8
Calcite	30 ± 10
Plagioclase	5 ± 2
Microcline	3 ± 1
Quartz	5 ± 2

TABLE 5

MODAL VOLUME PERCENT OF FRACTURE FILLING MINERALS
IN LOW-DIP FRACTURE ZONES (0- TO 150-m DEPTH)

Mineral	vol.%
Chlorite	12 ± 4
Muscovite/sericite	2 ± 0.5
Illite	21 ± 5
Iron oxides	20 ± 4
Calcite	5 ± 1
Biotite	5 ± 2
Plagioclase	8 ± 2
Microcline	12 ± 3
Quartz	15 ± 3

TABLE 6

MODAL VOLUME PERCENT MINERALS IN CORE URL5 AT 156.8 m
COMPARISON OF THREE METHODS OF ANALYSIS

Mineral	Modal Estimate	Modal Analysis	QUANTIMET*
Chlorite	15	17.5	19.5
Muscovite	2	1.6	-
Illite	20	18.8	23.5
Iron oxides	16	17.9	21.2
Calcite	1	1.5	3.
Biotite	1	1.5	1.2
Plagioclase	14	12.8	
Microcline	18	16.9	31.7*
Quartz	13	11.9	
Total	100	100	100

* QUANTIMET gives a total of quartz and feldspars.
It does not resolve into various phases.

TABLE 7

REPRESENTATIVE ANALYSES OF CHLORITES FROM THE WRA FRACTURE ZONES

	1	2	3	4
SiO_2	27.56	26.30	25.23	25.55
TiO_2	0.15	0.09	0.14	0.08
Al_2O_3	18.15	19.20	20.47	19.50
FeO	27.07	27.22	28.58	28.13
MnO	0.68	0.25	0.73	0.80
MgO	12.01	13.80	12.28	11.82
CaO	0.06	0.02	0.13	0.03
K_2O	0.08	0.14	0.07	0.01
Total	85.76	87.02	87.63	85.92

No. of cations based on 28 (0)

	1	2	3	4
Si	6.649	6.035	5.421	5.518
Ti	0.025	0.015	0.023	0.012
Al	4.861	4.624	5.183	5.023
Fe	4.870	4.894	5.182	5.058
Mn	0.122	0.045	0.135	0.140
Mg	4.418	3.872	3.934	3.866
Ca	0.014	0.004	0.024	0.007
K	0.022	0.038	0.020	0.002

All oxides expressed in weight percent.

TABLE 8

REPRESENTATIVE ANALYSES OF SERICITES AND ILLITES FROM FRACTURE ZONES IN THE WRA

| | Muscovite/Sericite | | | Illite | |
	1	2	3	1	4
SiO_2	48.59	46.04	46.65	54.88	55.51
TiO_2	0.51	0.54	0.47	0.07	0.05
Al_2O_3	28.85	29.92	30.60	19.02	20.11
FeU	4.44	5.66	4.82	0.02	0.05
MnO	0.05	0.00	0.01	0.02	0.05
MgO	2.42	3.11	2.21	2.00	1.82
CaO	0.22	0.38	0.36	0.56	0.77
Na_2O	0.61	0.34	0.04	0.15	0.33
K_2O	7.11	7.30	8.08	6.80	6.15
Total	92.80	93.34	93.29	83.88	86.45

No. of cations on the basis of 22 (O)

Si	6.700	6.307	6.371	7.878	7.835
Ti	0.051	0.056	0.048	0.008	0.005
Al	4.536	4.830	4.926	3.218	3.346
Fe	0.495	0.648	0.550	0.240	0.196
Mn	0.481	0.000	0.001	0.003	0.006
Mg	0.006	0.634	0.450	0.428	0.383
Ca	0.031	0.055	0.053	0.086	0.116
Na	0.158	0.090	0.010	0.041	1.090
K	1.210	1.275	1.407	1.246	1.108

All oxides expressed in weight percent.

TABLE 9

MODAL ANALYSES* OF GREY GRANITE
(From Stone et al. 1989)

Mineral	vol.%
Quartz	27.21 ± 2.55
Microcline	33.58 ± 3.68
Plagioclase	31.62 ± 4.11
Biotite	4.81 ± 2.10
Sphene	0.21 ± 0.15
Chlorite	0.31 ± 0.22
Epidote	0.52 ± 0.39
Muscovite	0.51 ± 0.40
Opaques	0.68 ± 0.33
Others	0.50 ± 0.41

* Based on point counting of 200 thin sections
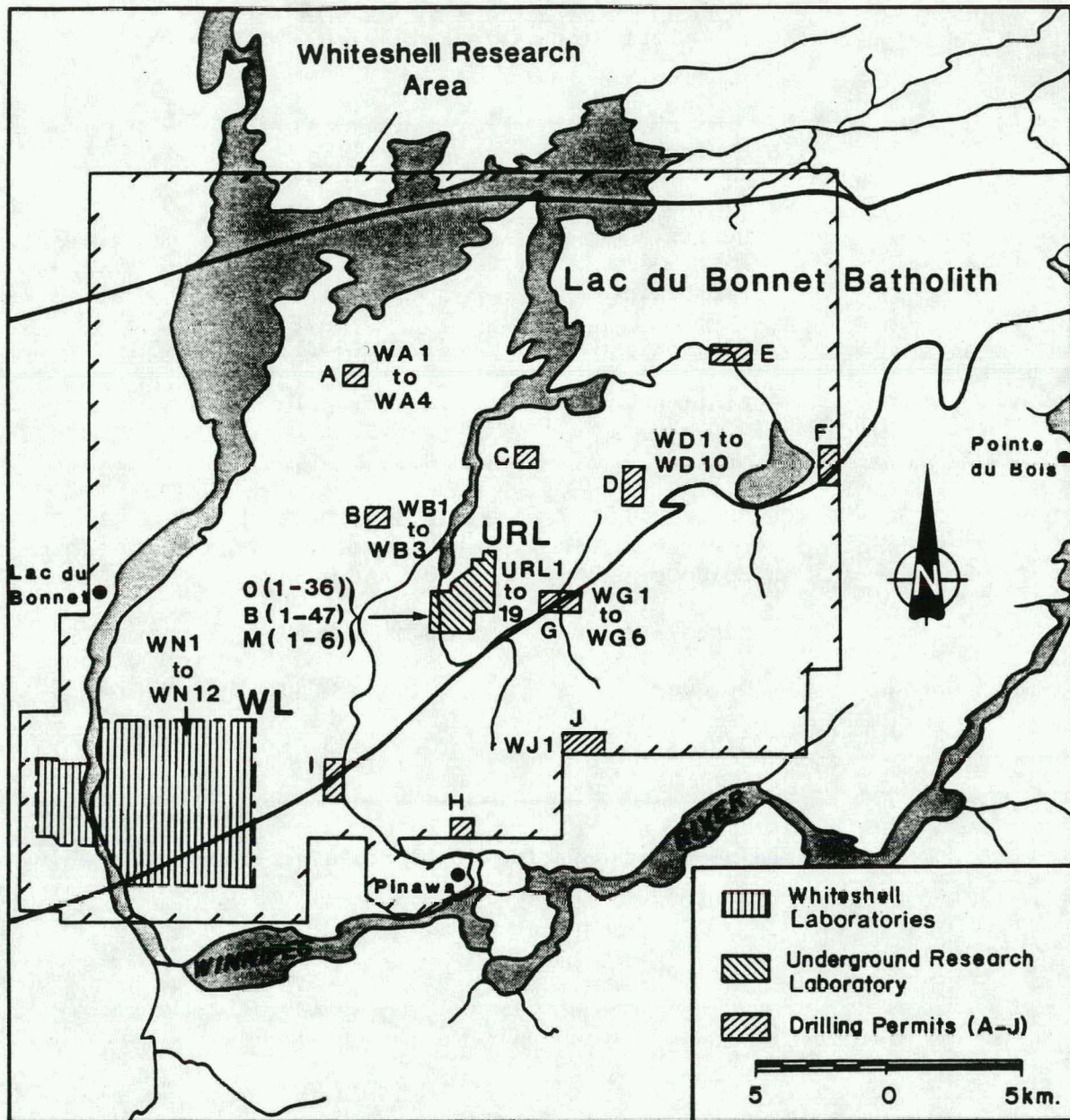
FIGURE 1: General Location of Borehole Sites Within the Whiteshell
Research Area
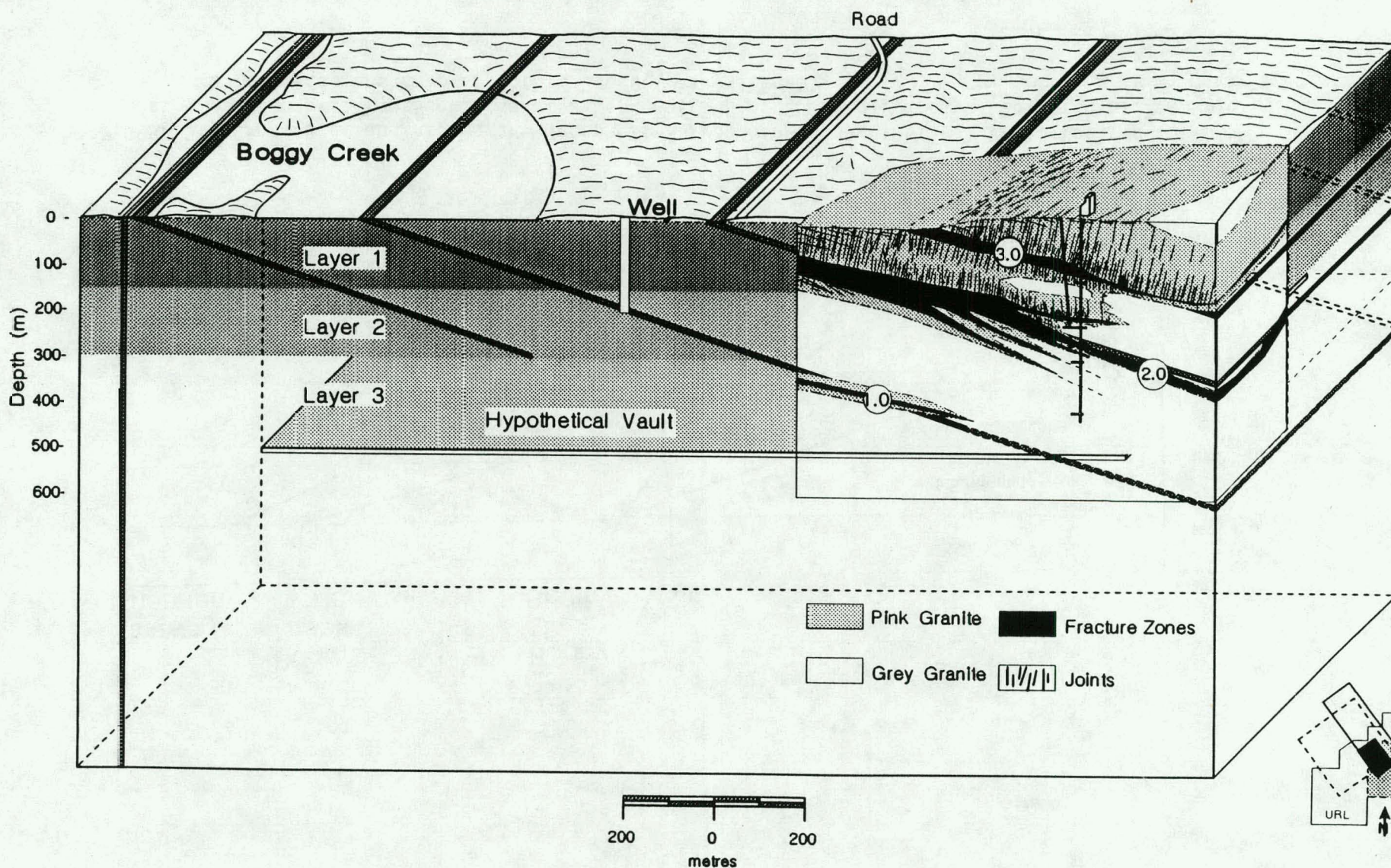
FIGURE 2: Interpretation of Geological Conditions at the URL Lease Area Showing a Representation of Groundwater Flow Paths along Numbered Fracture Zones, Locations of a Hypothetical Vault and Well and Modelled Rock Layers.
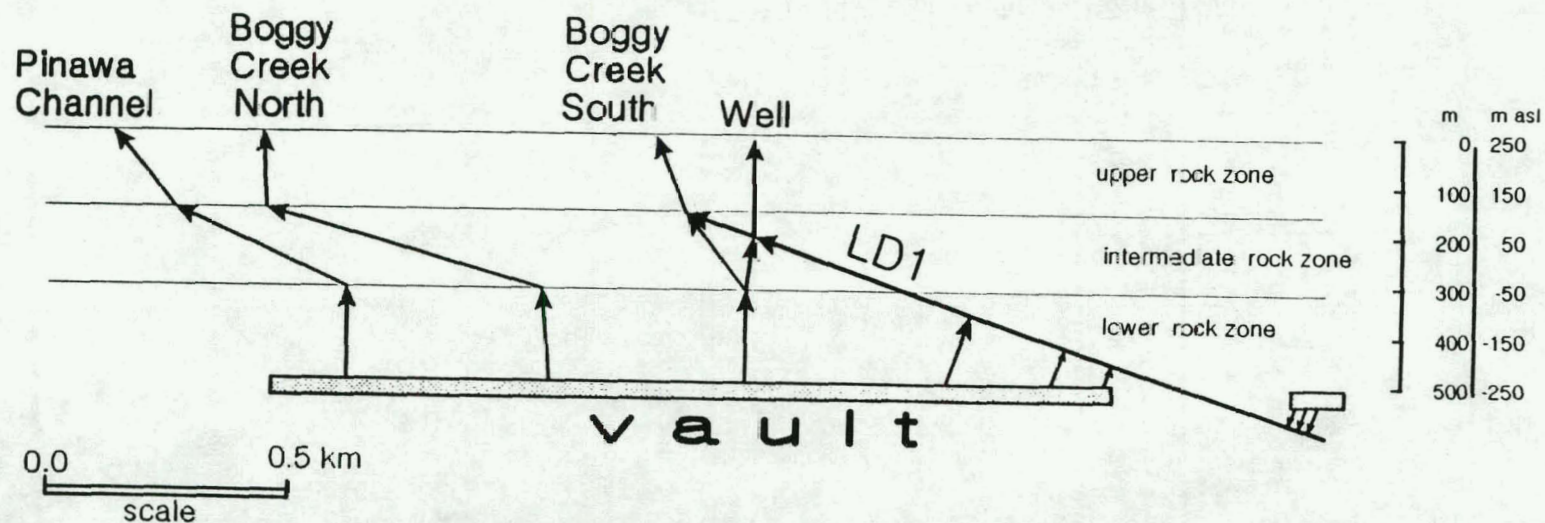
FIGURE 3: Cross Section Through the Geosphere Surrounding a Hypothetical Vault Located in the Whiteshell Research Area at a Depth of 500 m, Showing Principal Contaminant Pathways (Arrowed) and Major Fracture Zones (Dashed Lines)
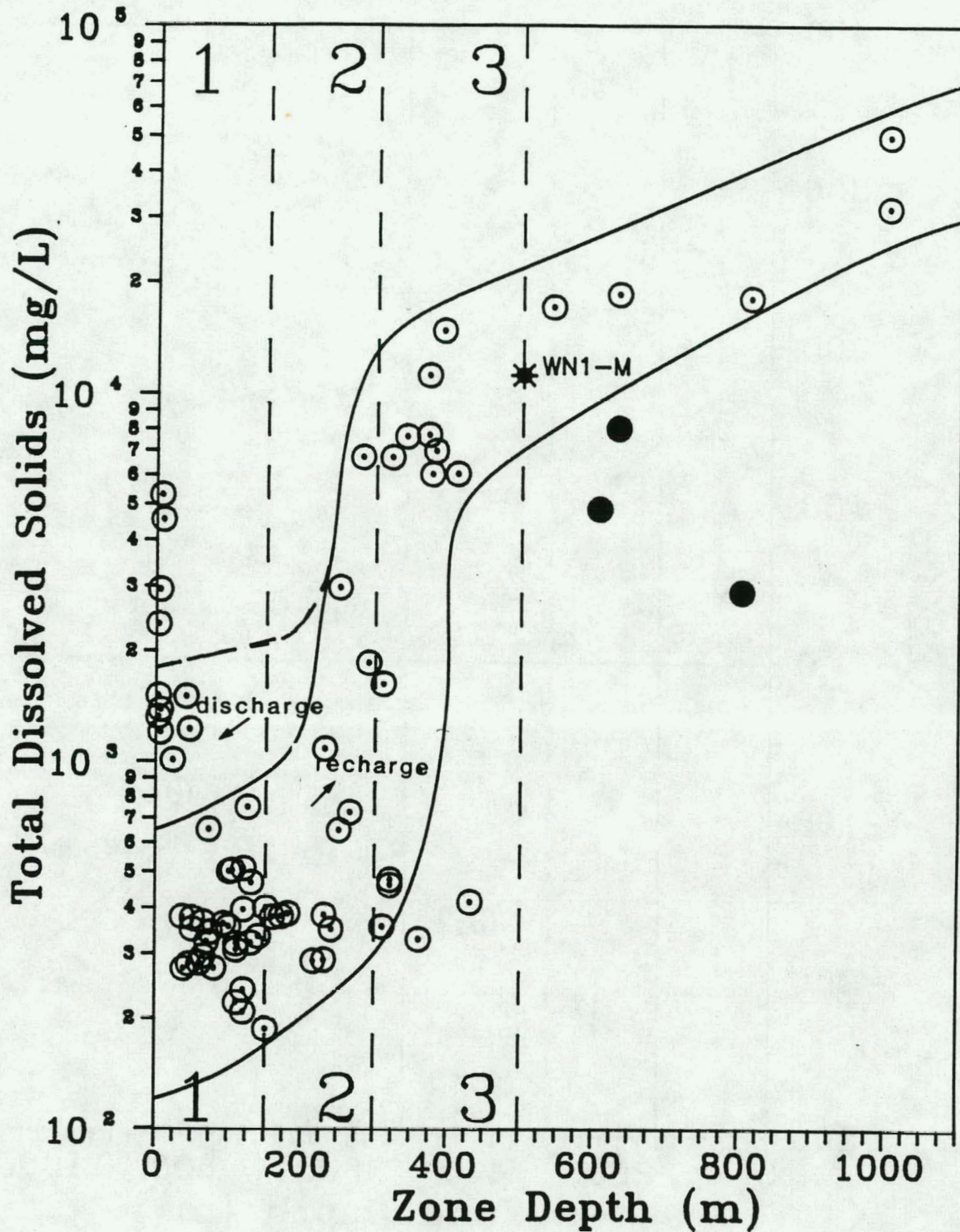
FIGURE 4: Variation of TDS with Depth for Groundwater from Fracture Zones in the Whiteshell Research Area. The rock layers upper, intermediate and lower are numbered 1, 2 and 3 respectively. The synthetic sample WN1-M is described in the text. Solid circles indicate samples contaminated with surface water.
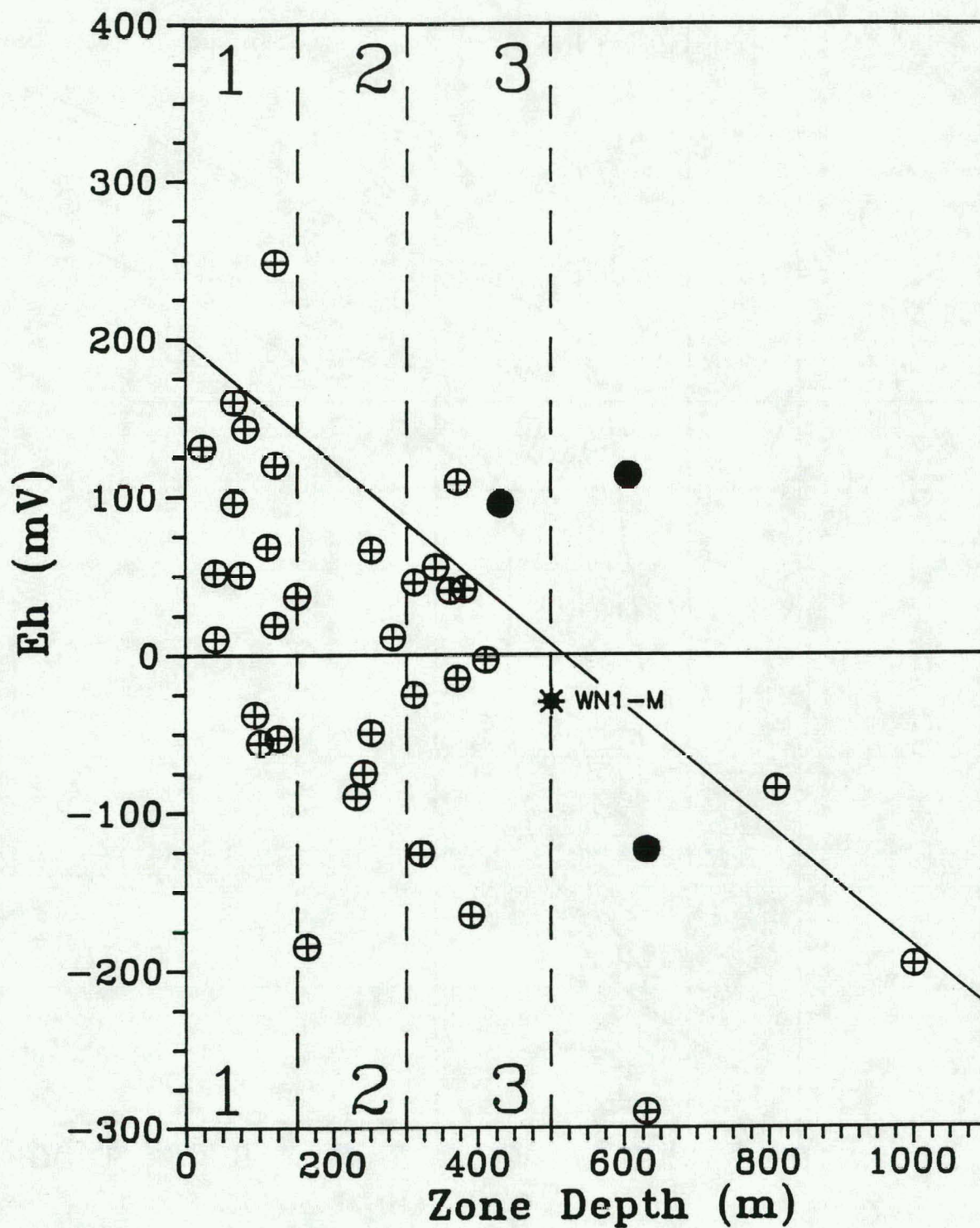
FIGURE 5: Variation of Redox Potential of Groundwaters in the Whiteshell Research Area with Depth. The rock layers upper, intermediate and lower are numbered 1, 2 and 3 respectively. The synthetic sample WN1-M is described in the text.

600

500

400

I (μg/L)

300

200

100

0

0   200   400   600   800   1000   1200
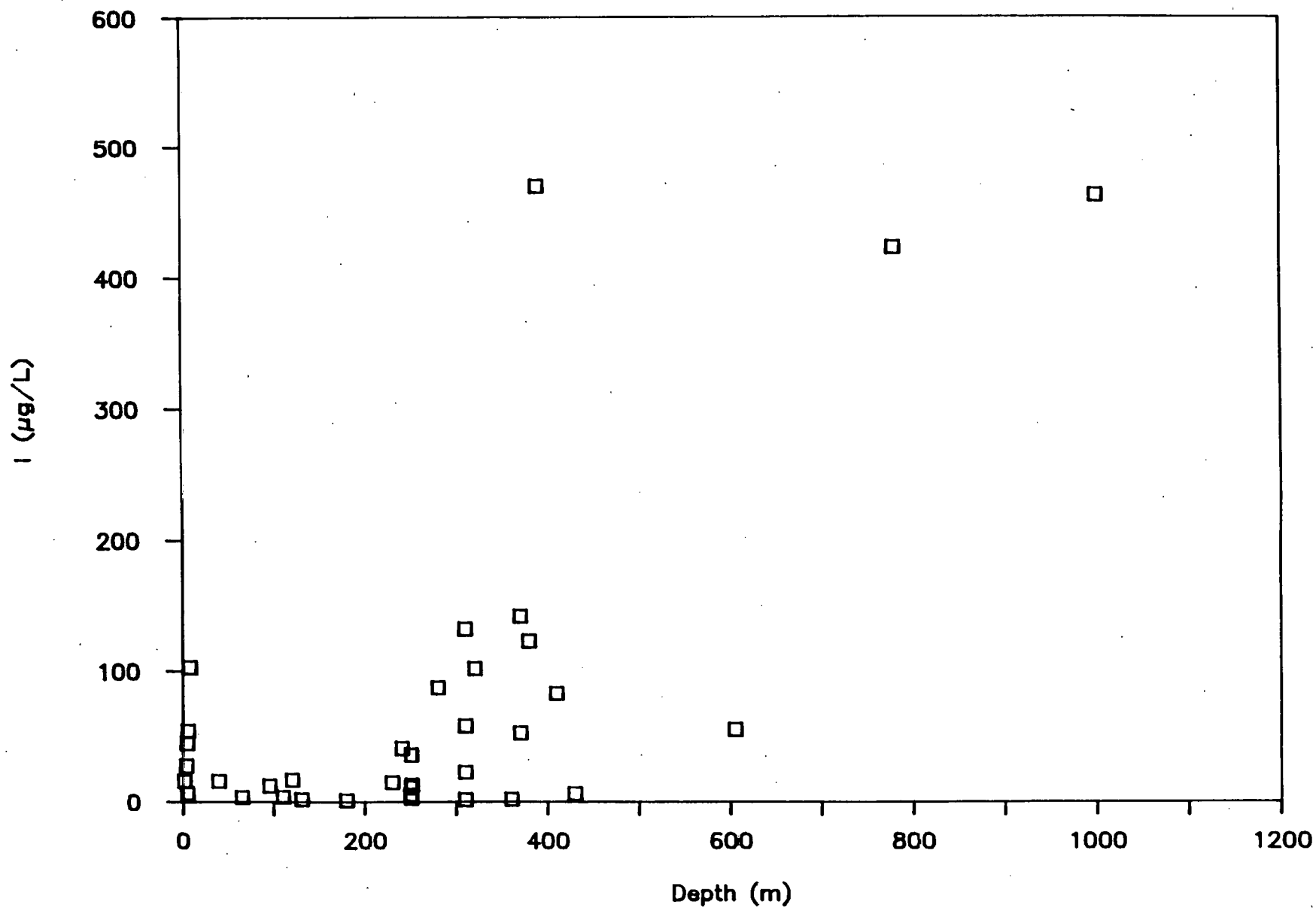
Depth (m)

FIGURE 6:   Variation of Iodide Concentration with Depth for WRA Groundwaters
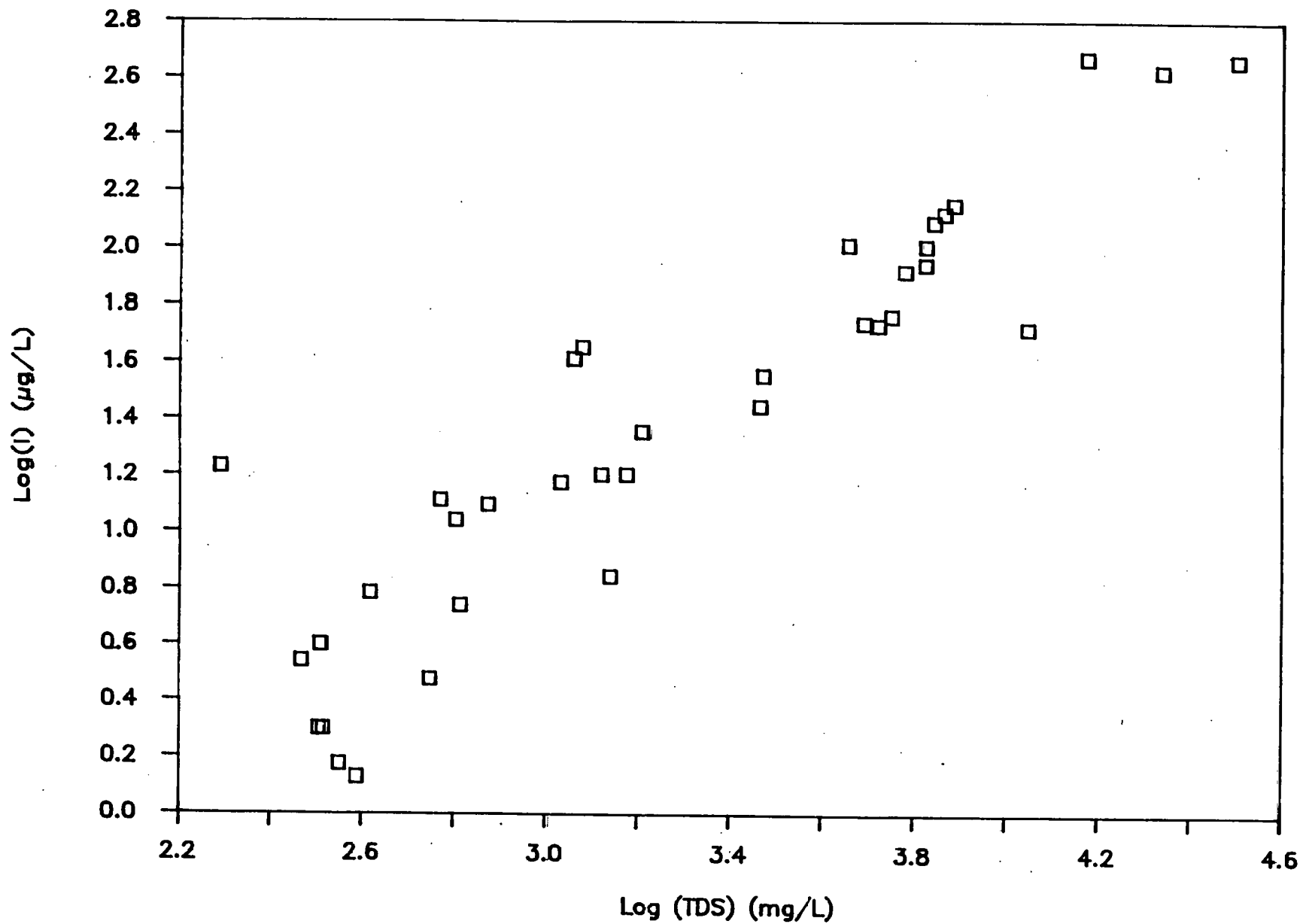
FIGURE 7: Variation of Iodide Concentration with Total Dissolved Solids for WRA Groundwaters